Atmos. Chem. Phys. Discuss., 10, 6713–6754, 2010
www.atmos-chem-phys-discuss.net/10/6713/2010/
© Author(s) 2010. This work is distributed under
the Creative Commons Attribution 3.0 License.

Atmospheric Chemistry and Physics Discussions

This discussion paper is/has been under review for the journal Atmospheric Chemistry and Physics (ACP). Please refer to the corresponding final paper in ACP if available.

Size distributions of dicarboxylic acids, ketoacids, α-dicarbonyls, sugars, WSOC, OC, EC and inorganic ions in atmospheric particles over Northern Japan: implication for long-range transport of Siberian biomass burning and East Asian polluted aerosols

S. Agarwal[1], **S. G. Aggarwal**[1,*], **K. Okuzawa**[1,**], **and K. Kawamura**[1]

[1]Institute of Low Temperature Science, Hokkaido University, Kita 19, Nishi 8, Sapporo – 0600819, Japan

* now at: National Physical Laboratory (Council of Scientific and Industrial Research), Dr. K.S. Krishnan Road, New Delhi – 110012, India
** now at: Japan Isotope Analysis Laboratory, Inc., 75-1 Onocho, Tsurumi-ku, Yokohama-city, Kanagawa 230-0046, Japan

Received: 25 February 2010 – Accepted: 28 February 2010 – Published: 10 March 2010

Correspondence to: K. Kawamura (kawamura@lowtem.hokudai.ac.jp)

Published by Copernicus Publications on behalf of the European Geosciences Union.

Abstract

To better understand the size-segregated chemical composition of aged organic aerosols in the western Pacific rim, day- and night-time aerosol samples were collected in Sapporo, Japan during summer 2005 using Andersen impactor sampler with 5 size bins: <1.1, 1.1–2.0, 2.0–3.3, 3.3–7.0, >7.0 µm. Samples were analyzed for the molecular compositions of dicarboxylic acids, ketoacids, α-dicarbonyls, and sugars, together with water-soluble organic carbon (WSOC), organic carbon (OC), elemental carbon (EC) and inorganic ions. Based on the analyses of backward trajectory and chemical tracers, we found that during campaign, the air masses were arrived from Siberia (biomass burning source region) on 8–9 August, China (anthropogenic source region) on 9–10 August and from the East China Sea/Sea of Japan (a mixed source receptor region) on 10–11 August. Most of the diacids, ketoacids, dicarbonyls, levoglucosan, WSOC, and inorganic ions, i.e., SO_4^{2-}, NH_4^+ and K^+ were enriched in fine particles ($PM_{1.1}$) whereas Ca^{2+}, Mg^{2+} and Cl^- peaked in coarse sizes (>1.1 µm). Interestingly, OC, most sugar compounds and NO_3^- showed bimodal distributions on fine and coarse modes. In $PM_{1.1}$, diacids in biomass burning-influenced aerosols from Siberia (mean: 252 ng m^{-3}) were more abundant than those in the aerosols from China (209 ng m^{-3}) and ocean (142 ng m^{-3}) whereas SO_4^{2-} concentrations maximized in the aerosols from China (mean: 3970 ng m^{-3}) followed by marine- (2946 ng m^{-3}) and biomass burning-influenced (1978 ng m^{-3}) aerosols. Higher loadings of WSOC (2428 ng m^{-3}) and OC (4358 ng m^{-3}) were found on the fine mode, where biomass-burning products such as levoglucosan is abundant. This paper presents a case study that biomass burning episodes in Siberian region have a significant influence on the chemical composition of carbonaceous aerosols in the western North Pacific rim.

ACPD

10, 6713–6754, 2010

1 Introduction

Tropospheric aerosols contain a significant quantity of organic components, which account for 10–70% of total fine aerosol mass (Jacobson et al., 2000; Kanakidou et al., 2005). Major sources of organic aerosols are associated with primary emissions from biomass burning and bio- and fossil-fuel combustions as well as secondary productions from biogenic and anthropogenic emissions (Claeys et al., 2004; Koch et al., 2007; Schichtel et al., 2008; Venkataraman et al., 2005; Wang et al., 2006a). Loadings of organic and inorganic aerosols are significantly influenced by biomass burning and other anthropogenic sources (Mochida et al., 2003; Wang et al., 2006a; Warneke et al., 2009). The changes in chemical compositions and their concentrations can lead to alter the optical and microphysical properties of aerosol particles (Reid et al., 1998).

Asian continent is one of the most important source regions for the emissions of natural dusts, pollutants and biomass burning aerosols on a global scale (Mochida et al., 2003; Simoneit et al., 2004a, b), which are long-range transported to the remote Pacific Ocean and North America (Brock et al., 2004). Therefore, the Asian aerosols have a potential impact on atmospheric chemistry and global climate forcing (Clarke et al., 2004; Huebert et al., 2003). The western North Pacific rim is a region where anthropogenic and mineral dust aerosols are flown from Asian continent to the remote Pacific region. Studies on aerosol characteristics in the western Pacific rim is of great importance to better understand the climate consequences linked with chemical and physical properties of the Asian aerosols over the Pacific region.

Biomass burning events in Siberia and South Asia mostly occur in late spring to summer (Warneke et al., 2009). During this period, dust episodes in Mongolian desert and loess regions of East Asia also contribute to the increased aerosol burden in the Pacific region (Clarke et al., 2004). In fact, on the pathways of Siberian biomass emissions toward North East Asia, dusts from Mongolian desert and loess regions provide an alkaline surface that uptakes acidic gas, adding more complexity to the Asian aerosols. Therefore, chemical compositions of aerosols influenced by these events are important

ACPD
10, 6713–6754, 2010

to better understand their atmospheric processing during a long-range transport in the western North Pacific rim.

Dicarboxylic acids and sugars are two major water-soluble compound classes that significantly contribute to water-soluble organic carbon (WSOC) in aerosol particles (Simoneit et al., 2004a, b; Wang et al., 2006b). In the ambient aerosols, dicarboxylic acids are mainly produced by photochemical processes (Kawamura and Yasui, 2005), while sugar compounds are derived from primary sources such as soil dust, biomass burning and biological activities (Fu et al., 2008 and references therein; Simoneit et al., 2004a, b). Therefore, their characterizations on molecular level can further strengthen the understanding on Asian outflows of aerosols. Some studies have been conducted in several Japanese Islands (especially southern area of the western Pacific rim) with a focus on the seasonal and temporal variations of Asian outflows (Clarke et al., 2004; Huebert et al., 2003 and references therein). However, the size distributions of organic aerosols at molecular level are rarely studied (Mochida et al., 2007), which can provide useful information on the sources and atmospheric processing of Asian aerosols.

In our previous paper, Aggarwal and Kawamura (2009) discussed an aging of WSOC fraction in total suspended particles (TSP) collected in Sapporo (northern Japan). In that study, we found that although organic carbon (OC) loading in aerosols may depend on sources, WSOC/OC ratios increased with the photochemical aging of aerosols. The increase in WSOC/OC ratios has been interpreted by a photochemical transformation of primary organic aerosols to WSOC and/or a formation of water-soluble secondary organic aerosol (SOA) via gas-to-particle conversion during long-range atmospheric transport. Although the size-segregated chemical compositions have not been studied in Sapporo (Aggarwal and Kawamura, 2009), such studies should provide helpful information to better understand atmospheric transformation processes.

In this study, we collected size-segregated aerosols in Sapporo, the western Pacific rim during summer on day- and night-time basis. Here, we analyzed the size-segregated aerosol samples for low molecular weight dicarboxylic acids, ketoacids, α-dicarbonyls, and sugar compound classes as well as WSOC, OC, EC and major

ACPD
10, 6713–6754, 2010

ions. Using air mass trajectory combined with tracer analyses, we found that 3 types of aged aerosols were sampled during campaign with an influence of biomass burning in Siberia, polluted aerosols from China, and marine + mixed source aerosols from the East China Sea/Sea of Japan. Here we report the size distributions of organic and inorganic species and discuss the influence of Siberian biomass burning and Chinese pollution episodes on the loading of organic aerosols in northern Japan. This size-segregated aerosol sampling followed by chemical analyses makes it possible to better discuss the atmospheric processing of water-soluble organic species.

2 Experimental

2.1 Aerosol sampling

The city of Sapporo (location: 43°3′56″ N and 141°21′27″ E, population: 1.9 million) is located in the western part of Hokkaido, the northernmost major island of Japan (see Fig. 1 in Aggarwal and Kawamura, 2009). It is a good location for collecting the long-range transported atmospheric particles from Siberia (Russia), China and surrounding seas (including the Sea of Japan and western North Pacific). Aerosol particles were segregated using Andersen high-volume impactor sampler with aerodynamic cut sizes at 1.1, 2.0, 3.3 and 7.0 µm (i.e., in 5 size bins: <1.1, 1.1–2.0, 2.0–3.3, 3.3–7.0, >7.0 µm; hereafter we discuss the size distributions considering these 5 size bins). Particles were collected on pre-combusted (at 450 °C for 6 h) quartz filters (30 cm diameter) and a backup quartz filter (20×25 cm) at a flow rate of ~566 L min^{-1}. Six sets of aerosol samples (and one set of field blank) were collected on the rooftop of our institute building (~15 m a.g.l.) At Hokkaido University. The samples were collected from 8 to 11 August on day- and night-time basis. Day-time samples were collected between 04:30 to 18:30 h (LT) whereas night-time samples were 19:30 to 03:30 h (LT). The filter samples were stored in a clean glass jar (pre-combusted) with a Teflon-lined screw cap at −20 °C prior to analysis.

ACPD
10, 6713–6754, 2010

2.2 Chemical analyses

Water-soluble dicarboxylic acids, ketocarboxylic acids and α-dicarbonyls in the aerosol filter samples were determined by the methods described elsewhere (Kawamura, 1993; Kawamura and Ikushima, 1993). Briefly, an aliquot of filter (one eighth of the Andersen filter, and ~5 cm^2 of backup filter) was cut off, and extracted with Milli-Q water (12–15 ml) using an ultrasonic bath (3×10 min). Organic acids and carbonyls in the extracts were derivatized to esters and acetals with 14% BF_3 in n-butanol, respectively. The derivatives were determined using a capillary gas chromatograph (GC). Recoveries of diacids in the analytical procedure were ~80% for oxalic acid and better than 80% for other species. Analytical errors in the determination of diacids were within 6% for major diacids based on duplicate analysis.

On the other hand, sugars were extracted from another aliquot of filter cut with a dichloromethane and methanol mixture (2:1), derivatized with N,O-bis-(trimethylsilyl)trifluoroacetamide (BSTFA), and determined using a GC/mass spectrometry (GC/MS) (Wang et al., 2006b). Recoveries of all sugar compounds determined during the analytical procedure were >90%, while the analytical errors were within 10% based on duplicate analysis.

For the measurement of water-soluble organic carbon (WSOC) and inorganic ions, an aliquot of filter (one eighth of the Andersen filter and ~5 cm^2 of backup filter) was extracted with organic-free Milli-Q water (>18 MΩ cm, 15 ml) using an ultrasonic bath for 30 min. Particles in the extracts were removed by filtration with quartz wool and then a membrane disc filter (Millex-GV, Millipore, 0.22 µm). For the determination of WSOC, 0.1 ml of 2 M hcl was added to 5 ml water extracts. After purging 10 min with ultra pure air (80 mL min^{-1}), 100 µL of solution were injected into a TOC analyzer (Shimadzu TOC-5000A) (Wang et al., 2005). Analytical errors were estimated to be within 6% by the duplicate analyses.

Another aliquot of water extracts (~7 ml) was used for the determination of major ions (i.e., SO_4^{2-}, NO_3^-, Cl^-, NH_4^+, K^+, Ca^{2+}, Mg^{2+} and Na^+) using a Metrohm-761 ion

ACPD
10, 6713–6754, 2010

chromatograph (IC). Anions were measured with a Shodex SI-90 4E column with an eluent of 1.8 mm Na_2CO_3+1.7 mm nahco$_3$. Cations were isolated on a Shodex YK-421 column with an eluent of 4 mm H_3PO_4. The anionic-IC was equipped with a suppressor, and a 4 mm H_2SO_4 solution was used to regenerate suppressor. Analytical errors were estimated to be 4% based on the duplicate analysis.

Organic and elemental carbon (OC and EC) were determined using a Sunset Lab carbon analyzer, following the Interagency Monitoring of Protected Visual Environments (IMPROVE) thermal evolution protocol and assuming carbonate carbon in the sample to be negligible. Typically, a 1.5 cm^2 punch of the filter was placed in a quartz boat inside the thermal desorption chamber of the analyzer, and then stepwise heating was applied (Wang et al., 2005). Analytical errors were estimated to be within 8% by the duplicate analyses of samples.

Concentrations of individual compounds, WSOC, OC, EC and inorganic ions reported here are all corrected for the field blanks.

2.3 Air mass back trajectories and fire spots

To characterize the air masses encountered at Sapporo during the campaign, 10-day back trajectory analysis was performed for each sample using the HYSPLIT4 model (http://www.arl.noaa.gov/ready/hysplit4.html, NOAA Air Resources Laboratory, Silver Spring, Maryland, United States). The backward trajectories were calculated for air masses starting from the sampling site (with sampling ending time) at 500 m height using the vertical velocity method and reanalysis data. The flow pattern was updated every 6 h.

Fire spots of biomass burning events from space were searched on the European Space Agency website (http://dup.esrin.esa.int/ionia/wfa). The satellite image shows dense hot spots in Siberia and South Asia from 29 July to 10 August 2005.

CC BY

3 Results and discussion

3.1 Characteristics of Sapporo aerosols, air mass types and origins

Chemical compositions of the Sapporo aerosols are largely influenced by continental outflows with lesser contributions of local emissions (Aggarwal and Kawamura, 2009). Figure 1 shows typical air mass trajectories obtained during the sampling period together with fire spots searched by satellite. The trajectories showed that during the campaign, we had encountered different air masses originated from Siberia (8–9 August), China (9–10 August) and the East China Sea/Sea of Japan (10–11 August), although fire spots were mostly observed in Siberian and South Asian regions.

To better identify the potential sources of aerosols originated from these regions, we used chemical tracers determined in $PM_{1.1}$ filter samples collected during the campaign (Fig. 2). For example, levoglucosan and K^+ are known as potential markers for biomass burning aerosols (Simoneit et al., 1999) whereas SO_4^{2-} is a marker for anthropogenic sources, and/or is an oxidation product of marine-derived dimethylsulfide (DMS) (De Bruyn et al., 1998). Similarly, major diacids are believed to form largely by photooxidation of organic precursors emitted from anthropogenic and biomass-burning sources (Kawamura and Ikushima, 1993; Kawamura and Yasui, 2005; Narukawa et al., 1999). EC is primarily emitted from combustion activities (Clarke et al., 2004). In our samples, levoglucosan, K^+, SO_4^{2-}, oxalic acid, phthalic acid and EC ranged from 2.6–20, 25–112, 1367–4481, 39–137, 5.8–13 and 110–719 ng m^{-3}, respectively. These tracers were used to strengthen the implications of air mass back trajectory analyses.

Aerosol samples collected on 8 August and 8–9 are characterized by high concentrations of levoglucosan and K^+ (Fig. 2), suggesting an influence from biomass burning. This is consistent with air mass trajectories calculated for these samples (Fig. 1), demonstrating that the air masses are delivered from Siberia, where hot spots of forest fires are observed. Thus these aerosols can be considered as biomass burning-influenced samples. In August 9 sample, high concentration of SO_4^{2-} (a potential an-

ACPD
10, 6713–6754, 2010

thropogenic source tracer) was obtained. The air masses for this sample travelled over Siberia and loess regions in East Asia, hence this sample can be regarded as pollution + biomass burning-influenced sample. Oxalic acid and EC also maximized in these samples (8 August, 8–9 and 9), further supporting that these samples are potentially influenced by biomass burning or pollution + biomass burning emissions. Similarly, relatively abundant SO_4^{2-} was detected in the 9–10 August sample (for which the source region was eastern China). This sample can be considered as pollution-influenced sample. Although K^+ is relatively abundant in this sample, concentration of levoglucosan is low, suggesting no significant contribution from biomass burning.

Moderate concentrations of SO_4^{2-} (a possible product of DMS oxidation) were found in 10 and 10–11 August samples (Fig. 2), suggesting an influence of marine sources. Interestingly, backward trajectory analyses show that air masses for these samples travelled across the East China Sea and Sea of Japan (Fig. 1). The air mass of 10–11 August sample was delivered through South Asia and southern Japan. The 10 August sample showed a peak of phthalic acid (formed by photooxidation of aromatics emitted from fuel combustion) and EC, indicating a possible influence of local emissions. On the other hand, phthalic acid and EC became lowest in the 10–11 August sample, although K^+, levoglucosan and oxalic acid are abundant. Therefore, this sample can be regarded as marine- + pollution- + biomass burning- (i.e., mixed sources) influenced sample. According to the information, each sample can be labelled to represent the influence of particular or mixed sources as summarized in Table 1.

3.2 Size distributions of dicarboxylic acids and related compounds

Characterizations of aerosol water-soluble organic carbon (WSOC) at molecular level are important to better understand their ability to act as CCN and estimate the hygroscopic growth factor of organics (Mcfiggans et al., 2005; Shilling et al., 2007). Dicarboxylic acids (diacids) are known as major water-soluble compound classes that affect the hygroscopic property of aerosols (Mcfiggans et al., 2005). Diacids are largely formed via photochemical processes. Their contributions to total aerosol carbon in-

CC BY

crease from the western Pacific rim to the central Pacific (Aggarwal and Kawamura, 2008; Kawamura and Sakaguchi, 1999). Therefore, their size-segregated compositions are useful to better understand the atmospheric processing of aerosols during transport (Mochida et al., 2007).

Saturated straight chain (C_2-C_{12}), branched chain and unsaturated dicarboxylic acids, midchain keto or hydroxy dicarboxylic acids (kc_3, kc_7, hc_4), ketoacids ($\omega c_2 - \omega C_9$, Pyr) and α-dicarbonyls (C_2-C_3) were determined in each stage of size-segregated aerosols. Their concentrations in fine, i.e., $PM_{1.1}$ (<1.1 μM) and coarse (>1.1 μM) particles are summarized in Table 2. Total concentrations of diacids ranged from 113–274 ng m^{-3} (mean: 201±56 ng m^{-3}) and 24–71 ng m^{-3} (45±12 ng m^{-3}) on fine and coarse modes, respectively. Oxalic acid (C_2) was found as the most abundant species with concentration range of 39–137 ng m^{-3} on fine mode (mean: 101±34 ng m^{-3}) and 7.2–32 ng m^{-3} on coarse mode (mean: 17±7.0 ng m^{-3}), followed by malonic (C_3) or succinic acid (C_4). Relative abundances of C_2, C_3 and C_4 in total diacids were 49±7.5, 18±0.9 and 13±2.4% on fine mode, and 38±6.5, 18±2.6 and 18±3.1% on coarse mode. Longer-chain diacids such as C_8, C_{11} and C_{12} were below the detection limit (ca. 0.005 ng m^{-3}) in some segregated aerosol fractions, probably due to the limited air volume for multiple stages.

It is important to note that diacid concentrations may be considerably varied depending on extraction and derivatization methods employed (Yang and Yu, 2008). For example, oxalic acid concentrations determined by organic solvent extraction followed by BSTFA derivatization and GC/MS measurement were found to be significantly lower (about 15 times) than those of oxalate determined by water extraction followed by IC measurement in $PM_{2.5}$ collected in Singapore (Yang and Yu, 2008). Further, oxalic and malonic acids were not detected and/or seriously depleted when organic solvent extraction/methyl ester derivatization techniques were employed for GC determination (Grosjean et al., 1979; Satsumabayashi et al., 1989). However, our method (water extraction followed by dibutyl ester derivatization and GC determination) proved that the recovery of oxalic acid is 80% as mentioned before. Kawamura and Barrie found

CC BY

a good correlation ($r = 0.84$) between the oxalic acid concentrations determined in the Arctic aerosols by IC and GC methods (unpublished results, 2002).

Size distributions of total diacids are shown in Fig. 3. The results demonstrate that concentrations of total diacids are maximized in fine particles ($PM_{1.1}$). Similar submicron maxima have been reported in the polluted urban air in Hungary (Krivácsy and Molnár, 1998) and in rural and urban sites in Hongkong (Yao et al., 2002). Other studies also showed the predominance of shorter-chain diacids in fine particles (Kawamura et al., 2007; Mochida et al., 2007; Narukawa et al., 2003). These findings are consistent with the hypothesis that low molecular weight diacids are the secondary oxidation products via gas-to-particle conversion in the atmosphere. This point is further discussed in Sect. 3.6.

The biomass burning (samples #1 and #2) or biomass burning + pollution (#3) aerosols showed higher concentrations of total diacids in $PM_{1.1}$ than those of pollution (#4), marine (#5) or marine + mixed sourced (#6) aerosols (Fig. 3). We found a strong correlation between oxalic acid and levoglucosan (a biomass burning tracer, the concentrations are discussed in Sect. 3.3) ($r = 0.94$), and between total diacids and levoglucosan ($r = 0.86$) in fine particles ($PM_{1.1}$). This suggests that possibly biomass burning is a potential source of diacids and their precursors. These results indicate that biomass burning episodes have a significant influence in northern Japan during the campaign. During biomass burning events, diacids can firstly be produced by thermal oxidation of biomass and be subsequently condensed onto pre-existing particles in the biomass burning plumes (Gao et al., 2003; Narukawa et al., 1999; Reid et al., 1998). Secondly, production of diacids via photochemical aging of intermediate smoke species (gas-to-particle conversion) in the atmosphere is another important pathway (Gao et al., 2003; Narukawa et al., 1999). Thirdly, production of diacids through aqueous phase reactions in aerosols may also be important (Sorooshian et al., 2006; Warneck, 2003).

Figure 4 shows individual concentrations of major diacid and ketoacid species detected in the size-segregated aerosol samples. Although diacids and ketoacids are generally more abundant in the fine size (<1.1 µm) than coarse sizes (>1.1 µm), they

CC BY

also exist in considerable amounts on coarse mode ($D_p > 1.1$ µm). In particular, azelaic acid (C_9) is abundantly present on coarse mode such as 3.3–7.0 µm or >7.0 µm in diameter (Fig. 4d). C_9 concentration is more abundant in coarse particles (>1.1 µM) than fine size (<1.1 µm) in all the sample sets (Table 2, Fig. 4d). The abundant presence of C_9 in coarse particles can be interpreted by heterogeneous oxidation of Δ9 double bond of unsaturated fatty acids such as oleic acid ($C_{18:1}$) and linoleic acid ($C_{18:2}$), which are derived from phytoplankton, higher plants and bacteria and are largely present in aerosols (Kawamura and Gagosian, 1987).

The loadings of diacids on coarse mode ($D_p > 1.1$ µm) are slightly higher than those on fine mode ($D_p < 1.1$ µm) in #5 and #6 samples, when the air mass types were categorized as marine or marine + mixed source (see Fig. 4). This suggests a possible association of diacids with sea-salt particles. Generally a shift of size maxima towards course mode is reported when aerosol particles get influenced with marine region (Huang et al., 2006; Neusüss et al., 2000). During the passage of air masses in the marine boundary layer, a change in the net concentrations of diacids in fine particles may in part occur due to their evaporation and subsequent deposition on the coarse particles that contain alkaline components. Mochida et al. (2003) also reported a shift of small diacids from submicrometer to supermicrometer sizes in coastal marine aerosols collected from the western North Pacific. Likewise Kerminen et al. (1999) found a concentration peak of diacids in supermicrometer size range in the lower Arctic aerosols. Ricard et al. (2002) reported that C_4 and C_5 diacids were abundant in coarse particles in the northern Finland aerosols when the air mass type was marine.

Concentrations of total ketoacids in the Sapporo aerosols ranged from 17–27 ng m^{-3} (mean: 23±3.4 ng m^{-3}) and 3.9–14 ng m^{-3} (7.5±2.3 ng m^{-3}) on fine and coarse modes, respectively (Table 2). Glyoxylic acid (ΩC_2) was found as the dominant ketoacid followed by 4-oxobutanoic acid (ΩC_4) and/or pyruvic acid (Pyr). Total concentrations of A-dicarbonyls ranged from 2.1–8.0 ng m^{-3} (mean: 4.8±2.2 ng m^{-3}) and 0.50–2.4 ng m^{-3} (1.3±0.50 ng m^{-3}) on fine and coarse modes, respectively. Being similar to diacids, concentrations of ketoacids and dicarbonyls also maximized on fine mode (Table 2).

ACPD
10, 6713–6754, 2010

It is of interest to note that these concentrations in fine particles were much more abundant in #1, #2 and #3 samples with an influence of biomass burning (Fig. 4). The correlation coefficients (r) of C_2 with ωC_2, Pyr and glyoxal (Gly) are 0.96, 0.90 and 0.87, respectively (obtained from all respective size-segregated aerosol concentrations). Considering the chemical equilibrium conditions, these strong correlations indicate that these species are important intermediates in the oxalic acid secondary formation pathways (Gly/Pyr$\rightarrow\omega C_2 \rightarrow C_2$) from the biogenic precursors (Aggarwal and Kawamura, 2008; Kawamura et al., 1996).

3.3 Size distributions of sugar compounds

Because sugars are water-soluble, they can influence the hygroscopic properties of aerosol particles (Mochida and Kawamura, 2004). Eight sugars (i.e., levoglucosan, fructose, glucose, sucrose, trehalose, mannitol, arabitol and inositol) were detected in the Sapporo aerosols. Their concentrations are given in Table 3. Total concentrations of sugars ranged from 5.6–31 ng m^{-3} (mean: 14±9.2 ng m^{-3}) and 1.9–74 ng m^{-3} (19±18 ng m^{-3}) in fine (<1.1 μm) and coarse (>1.1 μm) particles, respectively. Levoglucosan is the most abundant sugar in fine size ($PM_{1.1}$) (Table 3). However, other sugar compounds are more abundant than levoglucosan on coarse modes. Among them (on coarse mode), glucose and sucrose are most abundant on average (Table 3). Levoglucosan comprised 54±9.3% of total sugars on fine mode whereas it did only 2.5±0.95% on coarse mode. Instead, glucose and sucrose accounted for 23±1.9% and 20±7.8% of total sugars on coarse mode, respectively.

Levoglucosan (1,6-anhydro-β-D-glucopyranose), anhydrosaccharide, is a major pyrolysis product of cellulose, and is recognised as a tracer of biomass burning (Simoneit et al., 1999). It is considered to be resistant to degradation in the atmosphere and be generated by non-combustive processes, e.g., hydrolysis or microbial degradation of carbohydrates (Simoneit et al., 1999, 2000). Despite its usefulness in the source apportionment studies, very few studies were reported on the particle size distributions of levoglucosan (Fine et al., 2004; Herckes et al., 2006; Kleeman et al., 2008; Schkolnik et

CC BY

al., 2005). Figure 5 shows the size distributions of levoglucosan and total sugars during the campaign. Levoglucosan is enriched in fine particles with concentrations of 2.6–20 ng m^{-3} (mean: 7.8±6.2 ng m^{-3}), especially in biomass burning-influenced samples (#1 to #3), although its concentrations on coarse mode are very low (0.09–1.8 ng m^{-3}, 0.50±0.40 ng m^{-3}). These results are similar to the size distributions of levoglucosan reported in smoke impacted aerosol samples (Herckes et al., 2006; Schkolnik et al., 2005). This study indicates that biomass burning smoke is spread out over the Asian outflow region, and is impacting the air quality of the western North Pacific rim (Simoneit et al., 2004b).

On the other hand, other sugar species, i.e., primary saccharides including monosaccharides (glucose and fructose), disaccharides (inositol, sucrose and trehalose) and sugar polyols or reduced sugars (arabitol and mannitol) are found to exist mostly in coarse fractions. The size distributions of individual primary saccharides are shown in Fig. 6. They gradually show maximum concentrations in coarse sizes (>1.1 μM). The primary saccharides are derived by resuspension of surface soil and unpaved road dust (Simoneit et al., 2004c), which contain biological materials including fungi and bacteria.

Fructose shows bimodal distributions peaking at $PM_{1.1}$ and in coarse sizes (Fig. 6a, Table 3). Interestingly, its concentrations in $PM_{1.1}$ were found to be high in #1, #2, #3 and #6 samples (biomass burning and mixed aerosols), and well correlated with levoglucosan in $PM_{1.1}$ ($r = 0.83$). This relation likely suggests that fructose is in part emitted from biomass burning processes. Low to moderate concentrations of glucose were also found in fine particles in biomass burning-influenced samples, i.e., #1, #2 and #3 (Figure 6b). Fu et al. (2008) and references therein suggested that biomass burning is the primary source of glucose, fructose, galactosan and mannosan along with levoglucosan. Medeiros et al. (2006) also observed that wildfires strongly enhanced the emissions of uncombusted saccharides. Interestingly, inositol also shows bimodal distributions (Fig. 6c), being similar to fructose distributions. This again suggests its biomass burning sources.

CC BY

In contrast, arabitol and mannitol (reduced sugars) did not show any significant enrichment in fine particles (Fig. 6d and e). Their concentrations maximized in coarse sizes in all the sample sets (unimodal distributions), with higher concentrations in #1, #2 and #3 samples. Similarly, sucrose was found to be abundant in coarse particles (>7.0 µM) (Fig. 6f), and its maximum concentrations were found in #2 and #3 samples (moderately correlated ($r = 0.60$) to Ca^{2+} at coarse size >7.0 µM). Another disaccharide, trehalose is also enriched in coarse sizes (3.3–7.0 µM, >7.0 µM) with maximum concentration on 8–9 August (Fig. 6g). The disaccharides detected in coarse particles may be derived from the suspended soil dusts originated in Sapporo and/or Asian continent, where agriculture-tilling practices are the source for the emission of soil dusts into the passing aerosols (Simoneit et al., 2004b).

The elevated concentrations of sugar polyols (arabitol and mannitol) and trehalose on coarse mode may be attributed to biological sources like fungal spores (Yttri et al., 2007). During late summer, spores from fungi are most intensively emitted. Baueret et al. (2002) reported the diameters of smallest fungal spores of 2 µM, underlining their presence in the coarse sizes (i.e., 2.0–3.3, 3.3–7.0, >7.0 µm). They are also major soluble components in the bark of trees, branches and leaves (Medeiros et al., 2006). Coarse mode sucrose could also be associated with phloem of plants and developing leaves and flower buds (Bieleski, 1995) in addition to suspended soil dust and unpaved road dust. Further, small fractions of disaccharides and reduced sugars on fine mode detected in this study may be attributed to biomass burning (Fu et al., 2008 and references therein) or sources like pollens and some viruses (Yttri et al., 2007 and reference therein).

3.4 Size distributions of inorganic ions

Size distributions of inorganic ions (i.e., SO_4^{2-}, NH_4^+, K^+, NO_3^-, Ca^{2+}, Cl^-, and Mg^{2+}) determined in the aerosol samples are shown in Fig. 7. Results of Na^+ (sea-salt) are not given here because of possible artifact from glass containers used in this study. Total concentrations of inorganic ions ranged from 2031–6971 ng m^{-3}

CC BY

(mean: 4626±1618 ng m^{-3}) and 322–2588 ng m^{-3} (1024±630 ng m^{-3}) in fine and coarse aerosols, respectively. Among identified ions, SO_4^{2-} was found as the most abundant species, ranging from 1367–4481 ng m^{-3} (mean: 2965±1023 ng m^{-3}) on fine mode and 126–1605 ng m^{-3} (518±446 ng m^{-3}) on coarse mode. The second most abundant ion is NH_4^+, whose concentrations are 447–2372 ng m^{-3} (1459±627 ng m^{-3}) and 0.065–801 ng m^{-3} (248±210 ng m^{-3}) on fine and coarse modes, respectively. It is of interest to note that average molar ratios (NH_4^+/SO_4^{2-}) are >2 in both fine and coarse modes, suggesting that sulfate is neutralized by ammonium in the Sapporo aerosols. Ranges and mean concentrations of individual ions are summarized in Table 4.

SO_4^{2-} accounted for 64±1.6% and 45±14% of total inorganic ion mass on fine and coarse modes, respectively. Higher SO_4^{2-} concentrations were obtained on 9 August, 9–10 August and 10–11 August (Fig. 7a), when the air masses were transported from Asian continent. Although SO_4^{2-} is enriched in $PM_{1.1}$, substantial fractions of SO_4^{2-} were also found in the size intervals of 1.1–2.0 and 2.0–3.3 µM, possibly due to the coagulation of fine particles enriched with SO_4^{2-} in-cloud processes at different levels of relative humidity (Kerminen and Wexler, 1995; Zhao and Gao, 2008). Negligible fractions of SO_4^{2-} were found in larger coarse sizes (i.e., 3.3–7.0 and >7.0 µM), indicating that SO_4^{2-} does not associate with dust and sea-salt particles in our samples. Size distributions of NH_4^+ are comparable to those of SO_4^{2-}, and do not change significantly depending on the types of air masses (Fig. 7b). The correlation between NH_4^+ and SO_4^{2-} is very strong ($r = 0.99$) in $PM_{1.1}$ as well as in coarse sizes ($r = 0.97$, 0.99 and 0.93 for the size bins of 1.1–2.0, 2.0–3.3 and 3.3–7.0 µM, respectively), suggesting a presence of ammonium salt of SO_4^{2-}. The overall concentrations of NH_4^+ and SO_4^{2-} in biomass burning samples (#1 and #2) were lower than those in the pollution-influenced aerosol samples (#3 and #4).

K^+ is a useful tracer of biomass burning. Being consistent with levoglucosan, K^+ was most abundantly detected in fine particles ($PM_{1.1}$) in all the sample sets (Fig. 7c), again indicating the impact of biomass burning in this region. Considerable amounts of K^+

were also found on coarse modes of 1.1–2.0 and 2.0–3.3 µM. Because potassium salts are more hygroscopic in nature, such a size shift of potassium may be rather effective due to aging process of biomass burning aerosols (Huang et al., 2006). Minor amounts of K^+ detected on coarse modes of 3.3–7.0 and >7.0 µM are possibly derived from soil and sea-salt.

Interestingly, size distributions of NO_3^- showed two peaks at $PM_{1.1}$ and size bin >7.0 µm in most of the sample sets regardless the air mass types (Fig. 7d). Particulate NO_3^- on the coarse modes could have been formed from neutralization reactions of HNO_3 on sea-salt and soil dust particles (Herner et al., 2006; Zhuang et al., 1999). However, NO_3^- concentrations in our samples were rather low (range: 35–152 and 44–424 ng m^{-3}), which represented only 2.7±2.0 and 17±10% of total inorganic ion mass on fine and coarse modes, respectively. Both NO_3^- and EC (discussed in the following section) are tracers for fossil fuel burning, however low concentrations of NO_3^- relative to EC on fine modes (Table 4) are possibly due to the evaporative losses of NO_3^- during transport. Similar values (15–130 ng m^{-3}) of NO_3^- were reported in the western North Pacific for fine particles collected during spring, however, the concentrations of coarse mode (1700–5000 ng m^{-3}) were >10 times higher than those of fine mode (Mochida et al., 2007). Oxidation of NO_x to HNO_3 and the subsequent adsorption on salt/dust particles may be a responsible process for the higher concentrations of NO_3^- in the coarse mode.

Ca^{2+} (a potential indicator of mineral dust) maximized in coarse size (>7.0 µM) (Fig. 7e). Higher concentrations of Ca^{2+} were observed in #2, #3 and #5 samples. This is consistent with air mass trajectories, which show their passage over loess regions in China, the source regions of mineral dusts in East Asia. In #5 sample, the air masses came from the East China Sea, which is a receptor region of the dust/soil particles originated from Mongolia and Eastern China (Mochida et al., 2007; Simoneit et al., 2004b). Cl^- concentrations maximized at coarse sizes (Fig. 7f). Cl^- concentrations were very low, ranging from 3–16 ng m^{-3} and 21–107 ng m^{-3} on fine and coarse modes, respectively. Being similar to Cl^-, Mg^{2+} concentrations also maximized in

coarse sizes (Fig. 7g), suggesting a similar origin and source regions, i.e., sea salts.

3.5 Size distributions of WSOC, OC and EC

Size distributions of water-soluble organic carbon (WSOC), organic carbon (OC) and elemental carbon (EC) are shown in Fig. 8. Their concentrations are summarized in Table 4. EC was only detected on fine mode ($D_p < 1.1\,\mu m$). In all the sample sets, WSOC maximized in fine aerosols (mean: $1909 \pm 472\,ng\,m^{-3}$) (Fig. 8a). However, WSOC concentrations on fine modes of samples #1, #2 and #3 are about 30–60% higher than those of #4, #5 and #6 samples. This means that WSOC is enriched in biomass burning-influenced aerosols. Because WSOC is an important fraction of OC, high loadings of WSOC in biomass burning-influenced aerosols indicate that Siberian biomass burning events may significantly impact on air quality, aerosol physical and optical properties, and thus climate of the western North Pacific rim.

Although OC generally peaked in fine particles (Fig. 8b), a peak was also found in coarse particles. This bimodal distribution of OC may be a result of in-cloud processing of organic aerosols during long-range atmospheric transport. Alternatively, OC may be associated with sugar-related sources because this distribution pattern is similar to that of sugar compounds. As discussed above, possible source of sugars is soil resuspension (microorganisms and plant debris) that may also be an important source for OC loadings in coarse aerosols. However, by comparing OC concentrations in all the sample sets on fine or coarse modes or total concentrations (i.e., fine + coarse mode) separately, we found that OC is always higher in the biomass burning or biomass burning+ pollution aerosol samples. These results suggest that although soil resuspensions and atmospheric processes are potentially important for OC distributions on coarse mode, biomass burning is the major source that governs the OC loadings in the Sapporo aerosols during the summer campaign.

EC in $PM_{1.1}$ ranged from $110–719\,ng\,m^{-3}$ with a mean of $451 \pm 207\,ng\,m^{-3}$. This range and mean are about half of those (range: $620–1400\,ng\,m^{-3}$, mean:

ACPD
10, 6713–6754, 2010

840±340 ng m^{-3}) reported for fine aerosol particles (<1 μM) collected in spring during Asian dust season in the western North Pacific (Mochida et al., 2007). EC maximized in #3 sample (pollution + biomass burning) and minimized in #6 sample (marine + mixed sourced) (Fig. 8c). High EC concentration was also obtained in #5 sample when air masses were transported from marine region. Phthalic acid (Ph) (see Fig. 4e) and OC (see Fig. 8b) are both moderately enriched on fine mode of this sample. Because Ph is directly emitted from automobile exhausts (Kawamura and Kaplan, 1987) and also produced by a secondary photochemical oxidation of aromatic hydrocarbons emitted from fossil fuel combustions (Kawamura and Ikushima, 1993), this sample may consider as partially influenced by fossil fuel combustion of local origins.

3.6 Characteristic type of WSOC and OC in fine and coarse fractions

WSOC to OC ratios can be used to assess the photochemical aging of organics, especially in long-range transported aerosols such as Sapporo aerosols (Aggarwal and Kawamura, 2009). Figure 9a illustrates WSOC/OC ratios in size-segregated aerosols for all the sample sets. Except for #6 sample, WSOC/OC ratios peaked in fine particles. The ratios calculated for fine and coarse modes are 0.41–0.75 (mean: 0.55±0.12) and 0.10–0.72 (0.23±0.13), respectively. Similar results (~0.2–0.7) have been reported in different aerosol types (Duarte et al., 2007 and references therein). Further, high ratios (>0.4) were reported in aged aerosols, and biomass burning-influenced aerosols (Jaffrezo et al., 2005 and references therein). The oxidation of particulate organic matter during long-range transport should be responsible for high WSOC/OC ratios in aged aerosols as suggested in our previous study in Sapporo (Aggarwal and Kawamura, 2009). Although the concentrations of WSOC and OC are higher in biomass burning-influenced samples (#1, #2 and #3), a high WSOC/OC ratio is found in Chinese polluted aerosols (#4) possibly due to the low concentration of OC in this sample. A significant portion of OC may be oxidised to WSOC during transport to the western North Pacific rim from Asian continent.

ACPD
10, 6713–6754, 2010

Diacids are believed to be produced largely by secondary processes. In fact, smallest diacid (C_2) is proposed as end product of oxidative reactions of several longer-chain diacids and other organic precursors in the atmosphere (Aggarwal and Kawamura, 2008; Kawamura et al., 1996). Interestingly, size distributions of C_2 and total diacids, which showed a peak in $PM_{1.1}$, are quite similar to those of WSOC in all the sample sets (see Figs. 3, 4a and 8a). We found good correlations between C_2 (or C_2-C, i.e., carbon based concentrations) and WSOC ($r = 0.68$ (0.68)), and total diacids (or total diacid-C) and WSOC ($r = 0.81$ (0.85)) in $PM_{1.1}$, suggesting that a major portion of WSOC in fine particles is secondarily produced in both biomass burning and polluted plumes. However, the correlation coefficients are low and even negative in the coarse sizes. Furthermore, although C_2, total diacids and WSOC showed similar size distributions, their ratios, i.e., C_2/WSOC and total diacids/WSOC, are generally higher in $PM_{1.1}$ than those of coarse sizes in biomass burning- or/and pollution-influenced samples (Fig. 9b and c).

In contrast, size distributions of diacids and OC are not parallel in most of the samples (Fig. 3 and 8b). We found enhanced ratios of C_2-C/OC and total diacid-C/OC in $PM_{1.1}$, except for #5 and #6 samples (being similar to C_2/WSOC and total diacids/WSOC ratios), where the particles were influenced by marine sources (Fig. 9d and e). This can be interpreted by secondary photochemical production of diacids in the atmosphere. In the above two sets of samples, a shift of the mode peak towards larger size ranges was found, again suggesting that oxalic acid and other semivolatile species could have been adsorbed on alkaline sea-salt particles. The C_2-C/OC and total diacid-C/OC ratios are highest in the aerosol samples influenced by pollution sources (#4). Because WSOC accounted for more than 50% of OC in fine aerosols (except marine-influenced aerosols), this study indicates that a considerable fraction of OC on fine mode is likely formed by the secondary processes that occur in the atmosphere during long-range transport of organic precursors.

ACPD
10, 6713–6754, 2010

4 Summary and conclusions

Six sets of size-segregated (i.e., with 5 size bins: <1.1, 1.1–2.0, 2.0–3.3, 3.3–7.0, >7.0 µm) aerosol samples were collected on day- and night-time basis in Sapporo, northern Japan in summer 2005. Samples were analyzed for low molecular weight diacids, sugars, WSOC, OC and EC, as well as major ions. Chemical tracer analyses together with air mass backward trajectories demonstrated that, during the sampling periods, 3 different air masses encountered to Sapporo with an influence from Siberian biomass burning (8 August, 8–9 August), Chinese pollution (9 August, 9–10 August) and marine + mixed sources (10 August, 10–11 August). Major water-soluble organic compounds, i.e., diacids, peaked on fine mode ($D_p < 1.1$ µm). By comparing the size distributions, we conclude that diacids are more enriched in biomass burning-influenced samples than pollution- and marine-influenced aerosols. The high loadings of diacids and enhanced ratios of C_2-C/OC and diacid-C/OC in fine particles demonstrate that they are most likely produced by photochemical oxidation of organic precursors in the atmosphere during long-range transport. Biomass burning emissions are possibly a major source for diacids in the Sapporo aerosols during the campaign.

Levoglucosan showed maximum concentrations on fine mode in all the sample sets. They are several times more abundant in biomass burning-influenced samples. In contrast, other sugars peaked in coarse aerosols (>1.1 µm), although most sugars are more enriched in biomass burning-influenced aerosol samples. SO_4^{2-} (a dominant inorganic ion) showed maximum concentrations on fine mode. We found that it is more abundant in the samples influenced by Chinese aerosols. Ca^{2+} peaked mostly on coarse mode whereas NO_3^- showed bimodal distributions with a peak on fine and coarse modes. Higher OC loadings are observed in biomass burning aerosols than pollution aerosols. Similarly, WSOC that peaked on fine mode, showed a maximum concentration in biomass burning aerosols. We observed that WSOC and OC in fine aerosols are photochemically more processed in the atmosphere than those in coarse mode fractions. This study demonstrates that biomass-burning episodes in Siberia

ACPD
10, 6713–6754, 2010

have a significant influence on the carbonaceous aerosols in northern Japan and the western North Pacific rim.

Acknowledgements. This study is in part supported by the Japanese Ministry of Education, Science, Sport and Culture through grant-in-aid Nos. 17340166 and 19204055.

References

Aggarwal, S. G. and Kawamura, K.: Carbonaceous and inorganic composition in long-range transported aerosols over northern Japan: Implication for aging of water-soluble organic fraction, Atmos. Environ., 43, 2532–2540, 2009.

Aggarwal, S. G. and Kawamura, K.: Molecular distributions and stable carbon isotopic compositions of dicarboxylic acids and related compounds in aerosols from Sapporo, Japan: Implications for photochemical aging during long-range atmospheric transport, J. Geophys. Res., 113, D14301, doi:10.1029/2007JD009365, 2008.

Baueret, H., Kasper-Giebl, A., Löflund, M., Geibl, H., Hitzenberger, R., Zibuschka, F., and Puxbaum, H.: The contribution of bacteria and fungal spores to the organic carbon content of cloud water, precipitation and aerosols, Atmos. Res., 64, 109–119, 2002.

Beilesky, R. L.: Onset of phloem export from senescent petals of daylily, Plant Physiol., 109, 557–565, 1995.

Brock, C. A., Eatough, D., and Solomon, P. A.: Particle characteristics following cloud-modified transport from Asia to North America, J. Geophys. Res., 109, D23S26, doi:10.1029/2003JD004198, 2004.

Claeys, M., Graham, B., Vas, G., Wang, W., Vermeylen, R., Pashynska, V., Cafmeyer, J., Guyon, P., Andreae, M. O., Artaxo, P., and Maenhaut, W.: Formation of secondary organic aerosols through photooxidation of isoprene, Science, 303, 1173–1176, 2004.

Clarke A. D., Shinozuka, Y., Kapustein, V. N. et al.: Size distributions and mixtures of dust and black carbon aerosol in Asian outflow: Physiochemistry and optical properties, J. Geophys. Res., 109, D15S09, doi:10.1029/2003JD004378, 2004.

De Bruyn, W. J., Bates, T. S., Cainey, J. M., and Saltzman, E. S.: Shipboard measurements of dimethyl sulfide and SO_2 southwest of Tasmania during the first Aerosol Characterization Experiment (ACE 1), J. Geophys. Res., 103(D13), 16703–16711, 1998.

Duarte, R. M. B. O., Santos, E. B. H., Pio, C. A., and Duarte, A. C.: Comparison of structural features of water-soluble organic matter from atmospheric aerosols with those of aquatic humic substances, Atmos. Environ., 41, 8100–8113, 2007.

Fine, P. M., Chakrabarti, B., Krudysz, M., Schauer, J. J., and Sioutas, C.: Diurnal variations of individual organic compound constituents of ultra fine and accumulation mode particulate matter in the Los Angeles Basin, Environ. Sci. Technol., 38, 1296–1304, 2004.

Fu, P., Kawamura, K., Okuzawa, K., Aggarwal, S. G., Wang, G., Kanaya, Y., and Wang, Z.: Organic molecular composition and temporal variations of summertime mountain aerosols over Mt. Tai, North China Plain, J. Geophys. Res., 113, D19107, doi:10.1029/2008JD009900, 2008.

Gao, S., Hegg, D. A., Hobbs, P. V., Kirchstetter, T. W., Magi, B. I., and Sadilek, M.: Water-soluble organic components in aerosols associated with Savanna fires in Southern Africa: Identification, evolution, and distribution, J. Geophys. Res., 108(D13) 8491, doi:10.1029/2002JD002324, 2003.

Grosjean, D., Cauwenberghe, K. V., Schmid, J. P., Kelly, P. E., and Pitts Jr., J. N.: Identification of C3-C10 aliphatic dicarboxylic acids in airborne particulate matter, Environ. Sci. Technol., 12, 313–317, 1978.

Herckes, P., Engling, G., Kreidenweis, S. M., and Collett Jr., J. L.: Particle size distributions of constituents during the 2002 Yosemite aerosols characterization study, Environ. Sci. Technol., 40(15), 4554–4562, 2006.

Herner, J. D., Ying, Q., Aw, J., Gao, O., Chang, D. P. Y., and Kleeman, M.: Dominant mechanisms that shape the airborne particle size and composition in central California, Aerosol Sci. Technol., 40, 827–844, 2006.

Huang, X. F., Yu, J. Z., He, L. Y., and Yuan, Z.: Water-soluble organic carbon and oxalate in aerosols at a coastal urban site in China: Size distribution characteristics, sources, and formation mechanisms, J. Geophys. Res., 111, D22212, doi:10.1029/2006JD007408, 2006.

Huebert, B. J., Bates, T., Russell, P. B., Shi, G., Kim, Y. J., and Kawamura, K., Carmichael, G., and Nakajima, T.: An overview of ACE-Asia: Strategies for quantifying the relationships between Asian aerosols and their climatic impacts, J. Geophys. Res., 108(*D*23), 8633, doi:10.1029/2003JD003550, 2003.

Jacobson, M., Hansson, H.-C., Noone, K., and Charlson, R.: Organic atmospheric aerosols: Review and state of the science, Rev. Geophys., 38(2), 267–294, 2000.

Jaffrezo, J.-L., Aymoz, G., Delaval, C., and Cozic, J.: Seasonal variations of the water soluble

organic carbon mass fraction of aerosol in two valleys of the French Alps, Atmos. Chem. Phys., 5, 2809–2821, 2005, http://www.atmos-chem-phys.net/5/2809/2005/.

Kanakidou, M., Seinfeld, J. H., Pandis, S. N., Barnes, I., Dentener, F. J., Facchini, M. C., Van Dingenen, R., Ervens, B., Nenes, A., Nielsen, C. J., Swietlicki, E., Putaud, J. P., Balkanski, Y., Fuzzi, S., Horth, J., Moortgat, G. K., Winterhalter, R., Myhre, C. E. L., Tsigaridis, K., Vignati, E., Stephanou, E. G., and Wilson, J.: Organic aerosol and global climate modelling: a review, Atmos. Chem. Phys., 5, 1053–1123, 2005, http://www.atmos-chem-phys.net/5/1053/2005/.

Kawamura, K.: Identification of C_2-C_{10} ω-oxocarboxylic acids, pyruvic acid C_2-C_3 α-dicarbonyls in wet precipitation and aerosol samples by capillary GC and GC-MS, Anal. Chem., 65, 3505–3511, 1993.

Kawamura, K. and Kaplan, I. R.: Motor-exhaust emissions as a primary source for dicarboxylic acids in Los Angeles, Environ. Sci. Technol., 21, 105–110, 1987.

Kawamura, K. and Sakaguchi, F.: Molecular distributions of water-soluble dicarboxylic acids in marine aerosols over the Pacific Ocean including tropics, J. Geophys. Res., 104(D3), 3501–3509, 1999.

Kawamura, K. and Ikushima, K.: Seasonal change in the distribution of dicarboxylic acids in the urban atmosphere, Environ. Sci. Technol., 27, 2227–2235, 1993.

Kawamura, K. and Yasui, O.: Diurnal changes in the distribution of dicarboxylic acids, ketocarboxylic acids and dicarbonyls in the urban Tokyo atmosphere, Atmos. Environ., 39, 1945–1960, 2005.

Kawamura, K. and Gagosian, R. B.: Implications of ω-oxocarboxylic acids in the remote marine atmosphere for photo-oxidation of unsaturated fatty acids, Nature,325, 330–332, 1987.

Kawamura, K., Kasukabe, H., and Barrie, L. A.: Source and reaction pathways of dicarboxylic acids, ketoacids and dicarbonyls in Arctic aerosols: One year of observations, Atmos. Environ., 30, 1709–1722, 1996.

Kawamura, K., Narukawa, M., Li, S. M., and Barrie, L. A.: Size distributions of dicarboxylic acids and inorganic ions in atmospheric aerosols collected during polar sunrise in the Canadian high Arctic, J. Geophys. Res., 112, D10307, doi:10.1029/2006JD008244, 2007.

Kerminen, V.-M. and Wexler, A. S.: Growth laws for atmospheric aerosol particles: an examination of the bimodality of the accumulation mode, Atmos. Environ., 29, 3263–3275, 1995.

Kerminen, V.-M., Teinilä, K., Hillamo, R. E., and Mäkelä, T.: Size-segregated chemistry of

particulate dicarboxylic acids in the Arctic atmosphere, Atmos. Environ., 33, 2089–2100, 1999.
Kleeman, M. J., Riddle, S. G., and Jakober, C. A.: Size distribution of particle-phase molecular markers during a severe winter pollution episode, Environ. Sci. Technol., 42(17), 6469–6475, 2008.
Koch, D., Bond, T. C., Streets, D., Unger, N., and van der Werf, G. R.: Global impacts of aerosols from particular source regions and sectors, J. Geophys. Res., 112, D02205, doi:10.1029/2005JD007024, 2007.
Krivácsy, Z. and Molnár, Á.: Size distribution of ions in atmospheric aerosols, Atmos. Res., 46, 279–291, 1998.
Mcfiggans, G., Alfarra, M. R., Allan, J. D., Bower, K. N., Coe, H., Cubison, M., Topping, D.O., Williams, P. I., Decesari, S., Facchini, M. C., and Fuzzi, S.: Simplification of the representation of the organic component of atmospheric particulates, Faraday Discuss., 130, 1–22, doi:10.1039/b419435g, 2005.
Medeiros, P. M., Conte, M. H., Weber, J.C., and Simoneit, B. R. T.: Sugars as source indicators of biogenic organic carbon in aerosols collected above the Howland Experimental Forest, Maine, Atmos. Environ., 40(9), 1694–1705, 2006.
Mochida M., Kawamura, K., Umemoto, N., Kobayashi, M., Matsunaga, S., Lim, H.-J., Turpin, B. J., Bates, T. S., and Simoneit, B. R. T.: Spatial distributions of oxygenated organic compounds (dicarboxylic acids, fatty acids, and levoglucosan) in marine aerosols over the western Pacific and off the coast of East Asia: Continental outflow of organic aerosols during the ACE-Asia campaign, J. Geophys. Res., 108(D23), 8638, doi:10.1029/2002JD003249, 2003.
Mochida, M. and Kawamura, K.: Hygroscopic properties of levoglucosan and related organic compounds characteristic to biomass burning aerosols particles, J. Geophys. Res., 109, D21202, doi:10.1029/2004JD004962, 2004.
Mochida, M., Umemoto, N., Kawamura, K., Lim, H.-J., and Turpin, B. J.: Bimodal size distributions of various organic acids and fatty acids in the marine atmosphere: Influence of anthropogenic aerosols, Asian dusts, and sea spray off the coast of East Asia, J. Geophys. Res., 112, D15209, doi:10.1029/2006JD007773, 2007.
Narukawa, M., Kawamura, K., Anlauf, K. G., and Barrie, L. A.: Fine and coarse modes of dicarboxylic acids in the Arctic aerosols collected during the Polar Sunrise Experiment 1997, J. Geophys. Res., 108(D18), 4575, doi:10.1029/2003JD003646, 2003.
Narukawa, M., Kawamura, K., Takeuchi, N., and Nakajima, T.: Distribution of dicarboxylic acids

and carbon isotopic compositions in aerosols from 1997 Indonesian forest fires, Geophys. Res. Lett., 26, 3101–3104, 1999.
Neusüss, C., Pelzing, M., Plewka, A., and Herrmann, H.: A new analytical approach for size-resolved speciation of organic compounds in atmospheric aerosol particles: Methods and first results, J. Geophys. Res., 105(*D*4), 4513–4527, 2000.
Reid, J., Hobbs, P., Ferek, R., Blake, D., Martins, J., Dunlap, M., and Liousse, C.: Physical, chemical, and optical properties of regional hazes dominated by smoke in Brazil, J. Geophys. Res., 103(*D*24), 32059–32080, 1998.
Ricard, V., Jaffrezo, J.-L., Kerminen, V.-M., Hillamo, R. E., Teinilä, K., and Maenhaut, W.: Size distributions and model parameters of aerosol constituents in northern Finland during the European Arctic Aerosol Study, J. Geophys. Res., 107(D14), 4208, doi:10.1029/2001JD001130, 2002.
Satsumabayashi, H. Kurita, H., Yokouchi, Y., and Udeda, H.: Photochmeical formation of particulalate dicarboxylic acids under long-range transport in central Japan, Atmos. Environ., 24A, 1443–1450, 1990.
Schichtel B. A., Malm, W. C., Bench, G., Fallon, S., mcdade, C. E., Chow, J. C., and Watson, J. G.: Fossil and contemporary fine particulate carbon fractions at 12 rural and urban sites in the United States, J. Geophys. Res., 113, D02311, doi:10.1029/2007JD008605, 2008.
Schkolnik, G., Falkovich, A. H., Rudich, Y. , Maenhaut, W., and Artaxo, P.: New analytical method for the determination of levoglucosan, polyhydroxy compounds and 2-methylerythritol and its applications to smoke and rainwater samples, Environ. Sci. Technol., 39, 2744–2752, 2005.
Shilling, J. E., King, S. M., Mochida, M., Worsnop, D. R., and Martin, S. T.: Mass spectral evidence that small changes in composition caused by oxidative aging processes alter aerosol CCN properties, J. Phys. Chem. A, 111, 3358–3368, 2007.
Simoneit, B. R. T. and Elias, V. O.: Organic tracers from biomass burning in atmospheric particulate matter over the ocean, Mar. Chem., 69(3–4), 301–312, 2000.
Simoneit, B. R. T., Schauer, J. J., Nolte, C. G., Oros, D.R., Elias, V. O., Fraser, M. P., Rogge, W. F., and Cass, G. R.: Levoglucosan, a tracer for cellulose in biomass burning and atmospheric particles, Atmos. Environ., 33(2), 173–182, 1999.
Simoneit, B. R. T., Kobayashi, M., Mochida, M., Kawamura, K., and Huebert, B.J.: Aerosol particles collected on aircraft flights over the north-western Pacific region during the ACE-Asia campaign: Composition and major sources of the organic compounds, J. Geophys.

Res., 109, D19S09, doi:10.1029/2004JD004565, 2004a.
Simoneit, B. R. T., Kobayashi, M., Mochida, M., Kawamura, K., Lee, M., Lim, H.-J., Turpin, B. J., and Komazaki, Y.: Composition and major sources of organic compounds of aerosol particulate matter sampled during ACE-Asia campaign, J. Geophys. Res., 109, D19S10, doi:10.1029/2004JD004598, 2004b.
Simoneit, B. R. T., Elias, V. O., Kobayashi, M., Kawamura, K., Rushdi, A. I., Medeiros, P. M., Rogge, W. F., and Didyk, B. M.: Sugar-dominant water-soluble organic compounds in soils and characterization as tracers in atmospheric particulate matter, Environ. Sci. Technol., 38(22), 5939–5949, 2004c.
Sorooshian, A., Ashwani, R., Choi, H. et al.: Oxalic acid in clear and cloudy atmospheres: Analysis of data from International Consortium for Atmospheric Research on Transport and Transformation 2004, J. Geophys. Res., 111, D23S45, doi:10.1029/2005JD006880, 2006.
Venkataraman, C., Habib, G., Eiguren-Fernandez, A., Miguel, A. H., and Friedlander, S. K.: Residential biofuels in South Asia: Carbonaceous aerosol emissions and climate impacts, Science, 307, 1454–1456, 2005.
Wang, G. and Kawamura, K.: Molecular characteristics of urban organic aerosols from Nanjing: A case study of a mega-city in China, Environ. Sci. Technol., 39(19), 7430–7438, 2005.
Wang, G., Kawamura, K., Lee, S., Ho, K., and Cao, J.: Molecular, seasonal, and spatial distributions of organic aerosols from fourteen chinese cities, Environ. Sci. Technol., 40(15), 4619–4625, 2006b.
Wang, G., Kawamura, K., Watanabe, T., Lee, S., Ho, K., and Cao, J.: High loadings and source strengths of organic aerosols in China, Geophys. Res. Lett., 33, L22801, doi:10.1029/2006GL027624, 2006a.
Wang, H., Kawamura, K., and Shooter, D.: Carbonaceous and ionic components in wintertime atmospheric aerosols from two New Zealand cities: implication for solid fuel combustion, Atmos. Environ., 39, 5865–5875, 2005.
Warneck, P.: In-cloud chemistry opens pathway to the formation of oxalic acid in the marine atmosphere, Atmos. Environ., 37, 2423–2427, 2003.
Warneke, C., Bahreini, R., Brioude, J. et al.: Biomass burning in Siberia and Kazakhstan as an important source for haze over the Alaskan Arctic in April 2008, Geophys. Res. Lett., 36, L02813, doi:10.1029/2008GL036194, 2009.
Yang, L. and Yu, L. E.: Measurements of oxalic acid, oxalates, malonic acid, and malonates in atmospheric particulates, Environ. Sci. Technol., 42(24), 9268–9275, 2008.

Yao, X., Fang, M., and Chan, C. K.: Size distributions and formation of dicarboxylic acids in atmospheric particles, Atmos. Environ., 36, 2099–2107, 2002.
Yttri, K. E., Dye, C., and Kiss, G.: Ambient aerosol concentrations of sugars and sugar-alcohols at four different sites in Norway, Atmos. Chem. Phys., 7, 4267–4279, 2007, http://www.atmos-chem-phys.net/7/4267/2007/.
Zhao, Y. and Gao, Y.: Mass size distributions of water-soluble inorganic and organic ions in size-segregated aerosols over metropolitan Newark in the US east coast, Atmos. Environ., 42(18), 4063–4078, 2008.
Zhuang, H., Chan, C. K., Fang, M., and Wexler, A. S.: Size distributions of particulate sulfate, nitrate and ammonium at a coastal site in Hong Kong, Atmos. Environ., 33, 843–853, 1999.

Table 1. Description of air mass types, source regions, and their passages for the Sapporo aerosol samples collected in summer 2005.

Sample ID	Sampling date	Air mass types	Origin and passage
#1	8 August and	Biomass burning	Siberia (lake Baikal and
#2	8–9 August		Asian loess regions)
#3	9 August	Pollution+biomass burning	Siberia, north-east China (Asian loess regions)
#4	9–10 August	Pollution	Eastern China, East China Sea
#5	10 August	Marine	East China Sea, Sea of Japan
#6	10–11 August	Marine + mixed sources (i.e., pollution and biomass burning)	South Asia, southern Japan, East China Sea, Sea of Japan

Table 2. Concentrations (ng m^{-3}) of dicarboxylic acids, ketoacids and dicarbonyls in the size-segregated aerosols from Sapporo, northern Japan.

Compounds	Fine mode (D_p <1.1 μM) Range	Fine mode (D_p <1.1 μM) Mean±SD	Coarse mode (D_p >1.1 μM) Range	Coarse mode (D_p >1.1 μM) Mean±SD
		Dicarboxylic acids		
		Saturated Straight Chain Diacids		
Oxalic, C_2	39–137	101±34	7.2–32	17±7.0
Malonic, C_3	20–48	35±9.1	3.2–13	8.1±2.5
Succinic, C_4	20–33	25±4.6	5.1–12	7.7±1.7
Glutaric, C_5	0.76–6.8	4.2±2.6	0.27-2.8	1.7±0.70
Adipic, C_6	1.8–4.7	3.4±1.3	0.57–1.4	0.93±0.24
Pimelic, C_7	0.12–0.38	0.22±0.10	0.06–0.35	0.15±0.08
Suberic, C_8	BDL	BDL	BDL-0.55	0.23±0.15
Azelaic, C_9	1.2–2.7	1.8±0.61	0.33–2.0	0.81±0.35
Sebacic, C_{10}	0.53–2.3	1.3±0.64	0.04–0.33	0.14±0.07
Undecanedioic, C_{11}	BDL-2.1	1.1±0.94	BDL-0.40	0.12±0.12
Dodecanedioic, C_{12}	BDL-0.11	0.03±0.05	BDL±0.03	0.01±0.01
		Unsaturated Diacids		
Maleic, M	1.4–3.4	2.3±0.91	0.49-1.3	0.80±0.17
Fumeric, F	0.31–1.6	0.87±0.51	0.18–0.65	0.33±0.14
Methylmaleic, mm	1.1–2.7	1.6±0.60	0.27-1.2	0.60±0.21
Phthalic, Ph	5.8–13	10±2.8	0.81–7.3	2.8±1.4
Iso-phthalic, iph	0.10–1.5	0.50±0.48	0.04–0.39	0.14–0.08
Tere-phthalic, tph	BDL-3.1	1.3±1.5	BDL-0.59	0.25-0.18
		Branched Chain Diacids		
Methylmalonic, ic_4	0.57–1.2	0.77±0.29	0.11–0.82	0.48–0.18
Methylsuccinic, ic_5	0.49–1.4	0.92±0.33	0.15–0.75	0.38±0.16
Methylgluteric, ic_6	1.4–3.4	2.3–0.91	0.49–1.3	0.80±0.17
		Keto or Hydroxy Diacids		
Malic, hc_4	BDL-0.26	0.09±0.13	0.04-0.37	0.16±0.10
Oxomalonic, kc_3	1.2–6.6	3.5±2.2	0.2–1.9	0.72±0.40
4-Oxopimelic, kc_7	1.2–8.2	5.1±2.8	0.16–1.4	0.56±0.40
Total diacids	113–274	201±56	24–71	45±12
		Ketoacids		
Pyruvic, Pyr	2.4–8.0	4.8±2.2	0.46–1.6	1.1±0.33
Glyoxylic, ωC_2	7.7–15	12±3.4	1.0–3.6	1.9±0.69
3-Oxopropanoic, ωC_3	BDL-0.21	0.07±0.09	BDL-0.27	0.15±0.08
4-Oxobutanoic, ωC_4	0.32–9.9	4.6±3.9	0.71–10	4.2±2.3
9-Oxononanoic, ωC_9	BDL-4.2	1.3±1.6	BDL-0.73	0.14±0.19
Total ketoacids	17–27	23±3.4	3.9-14	7.5±2.3
		α-Dicarbonyls		
Glyoxal, Gly	0.85–3.2	1.8±0.77	BDL-0.71	0.40±0.17
Methylglyoxal, megly	0.26–4.8	2.9±1.7	0.25–1.7	0.91±0.40
Total dicarbonyls	2.1–8.0	4.8±2.2	0.50-2.4	1.3±0.50

BDL= below detection limit (ca. 0.005 ng m^{-3}).

ACPD
10, 6713–6754, 2010

Table 3. Concentrations (ng m^{-3}) of sugar compounds in the size-segregated aerosols from Sapporo, northern Japan.

Compounds	Fine mode ($D_p < 1.1$)		Coarse mode ($D_p > 1.1$)	
	Range	Mean±SD	Range	Mean±SD
Levoglucosan	2.6–20	7.8±6.2	0.09–1.8	0.50±0.40
Fructose	1.1–4.1	2.1±1.2	0.19–5.7	1.3±1.6
Glucose	0.50–3.4	1.7±1.1	0.29–14	4.2±3.9
Sucrose	0.10–1.5	0.69±0.49	0.07–26	3.9±7.1
Trehalose	0.10–0.55	0.28±0.19	0.21–19	3.3±4.8
Mannitol	0.10–1.4	0.69±0.50	0.17–11	3.3±2.9
Arabitol	0.10–0.89	0.35±0.29	0.12–6.1	2.0±1.7
Inositol	0.10–0.49	0.29±0.14	0.02–0.40	0.10±0.10
Total sugars	5.6–31	14±9.2	1.9–74	19±18

CC BY

Table 4. Concentrations (ng m^{-3}) of WSOC, OC, EC and major ions in the size-segregated aerosols from Sapporo, northern Japan.

Major constituents	Fine mode ($D_p < 1.1$)		Coarse mode ($D_p > 1.1$)	
	Range	Mean±SD	Range	Mean±SD
WSOC	1385–2542	1909±472	297–699	452±126
OC	1850–4725	3563±954	412–4679	2390±1093
EC	110–719	451±207		
SO_4^{2-}	1367–4481	2965±1023	126–1605	518±446
NO_3^-	35–152	102±51	44–424	138±87
Cl^-	3–16	7±5	21–107	43±23
NH_4^+	447–2372	1459±627	65–801	248±210
K^+	25–112	71±28	7–58	23±11
Ca^{2+}	12–37	21±9	17–200	54±47
Mg^{2+}	1–5	3±2	3–13	6±3
Total inorganic ions	2031–6971	4626±1618	322–2588	1024±630

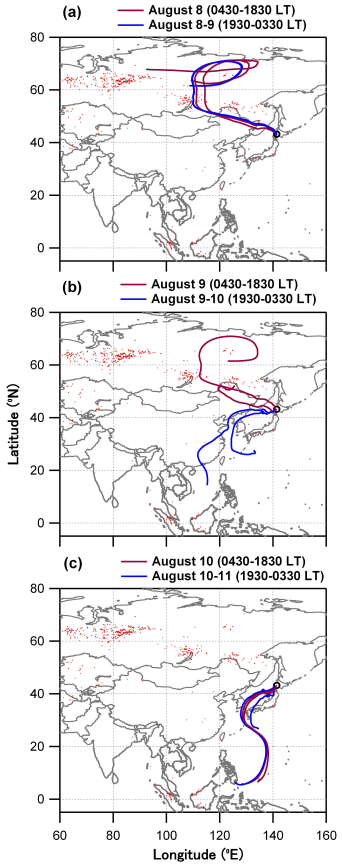

Fig. 1. 10-day air mass backward trajectory analysis results (see Table 1 for the details on air mass types, source regions and their passages for each samples collected during the campaign from 8–11 August 2005 in Sapporo, northern Japan) overlaid the fire spots searched by the satellite over Siberia and Asia, which were obtained from the European Space Agency website (http://dup.esrin.esa.int/ionia/about_ionia.asp), from 29 July to 10 August.

ACPD
10, 6713–6754, 2010

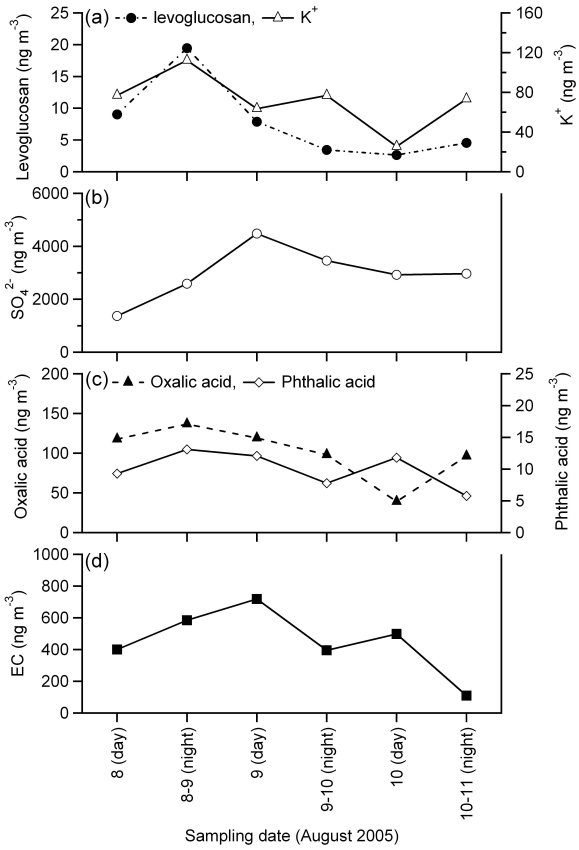

Fig. 2. Concentrations of some marker species determined in fine particles ($PM_{1.1}$) during the campaign from 8–11 August 2005.

ACPD
10, 6713–6754, 2010

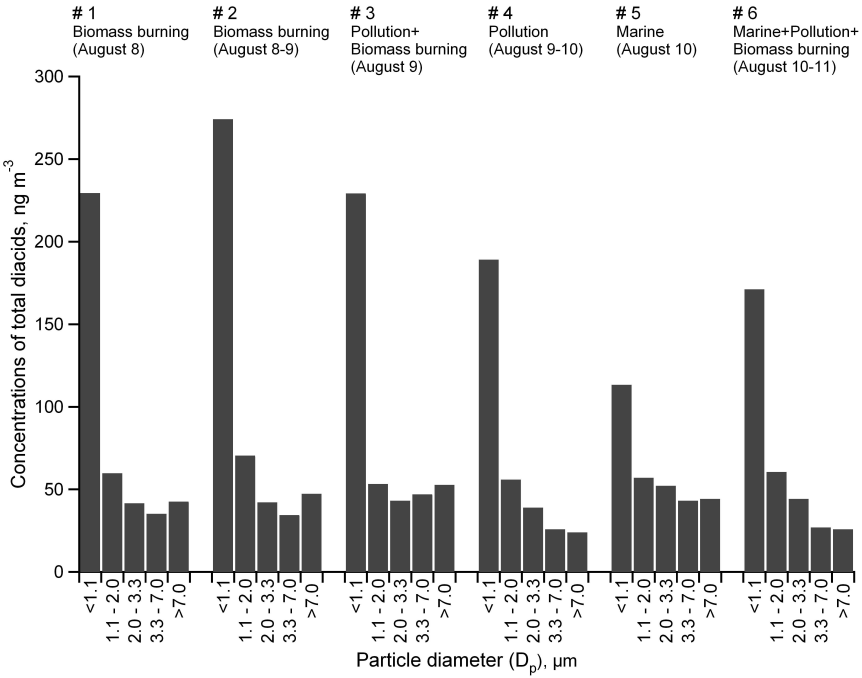

Fig. 3. Size distributions of total diacids in the Sapporo aerosols collected in summer, 2005.

ACPD
10, 6713–6754, 2010

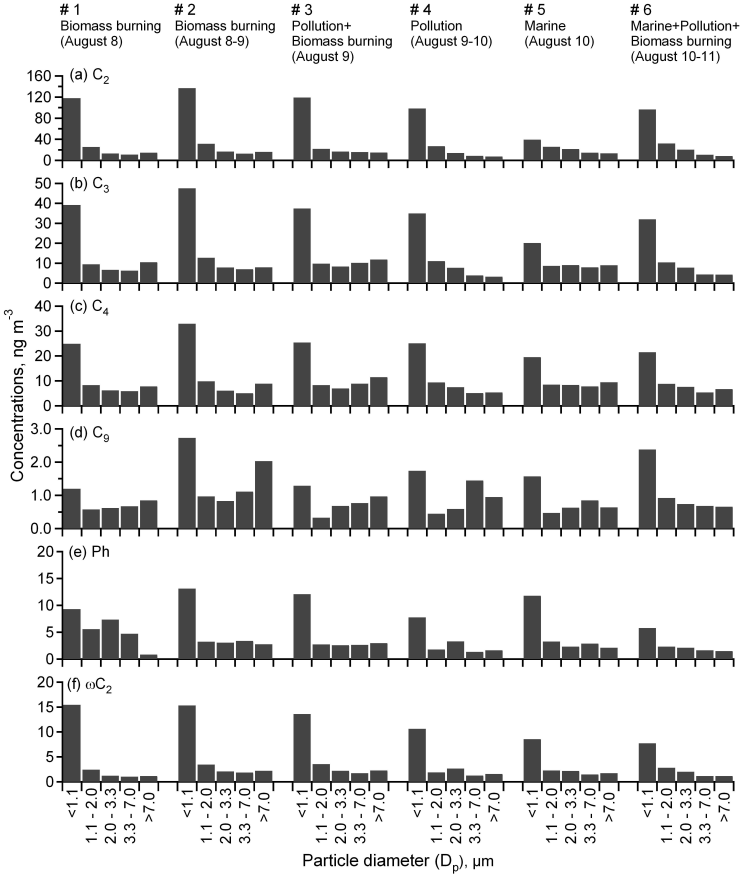

Fig. 4. Size distributions of major diacids and ketoacid in the Sapporo aerosols collected in summer, 2005.

ACPD
10, 6713–6754, 2010

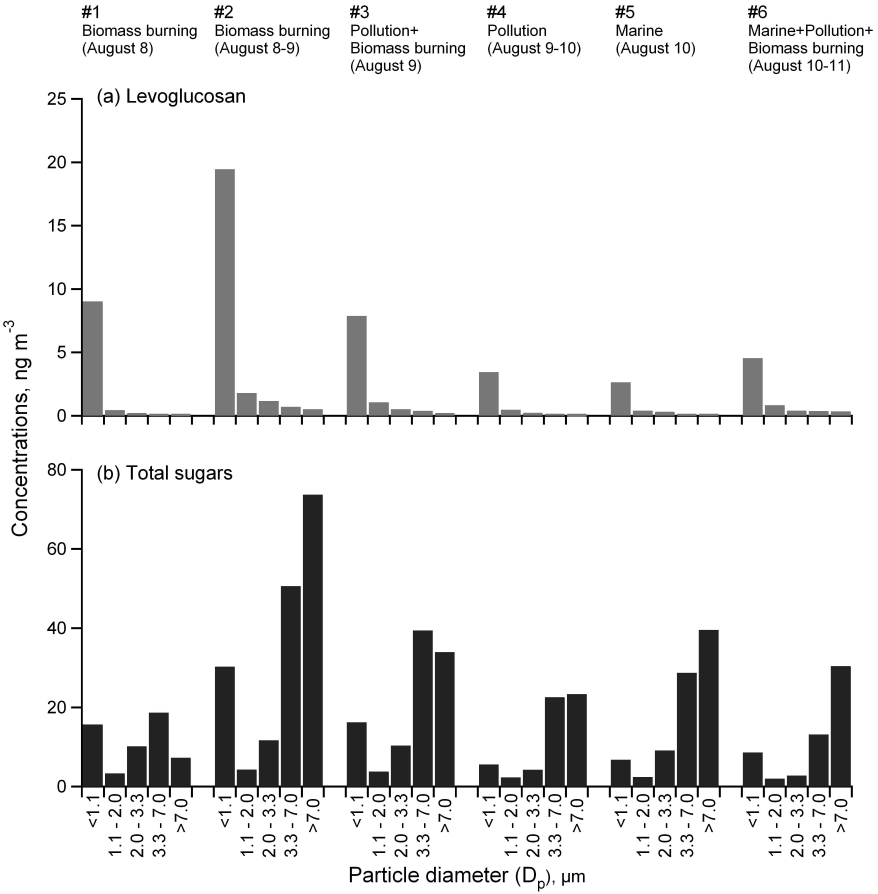

Fig. 5. Size distributions of **(a)** levoglucosan and **(b)** total sugars in the Sapporo aerosols collected in summer, 2005.

ACPD
10, 6713–6754, 2010

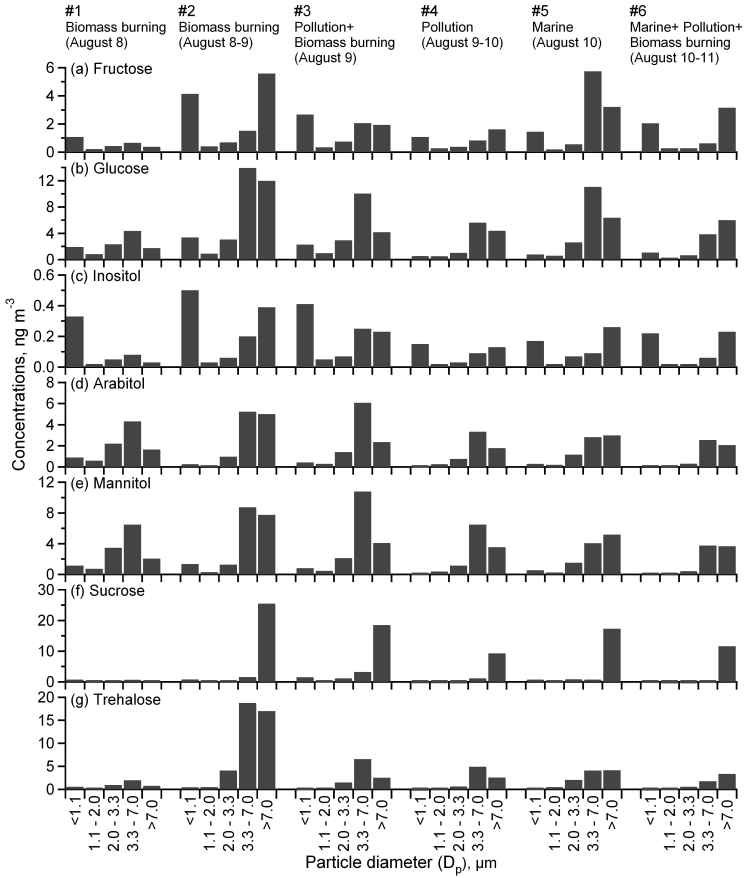

Fig. 6. Size distributions of individual sugar compound classes in the Sapporo aerosols collected in summer, 2005.

ACPD
10, 6713–6754, 2010

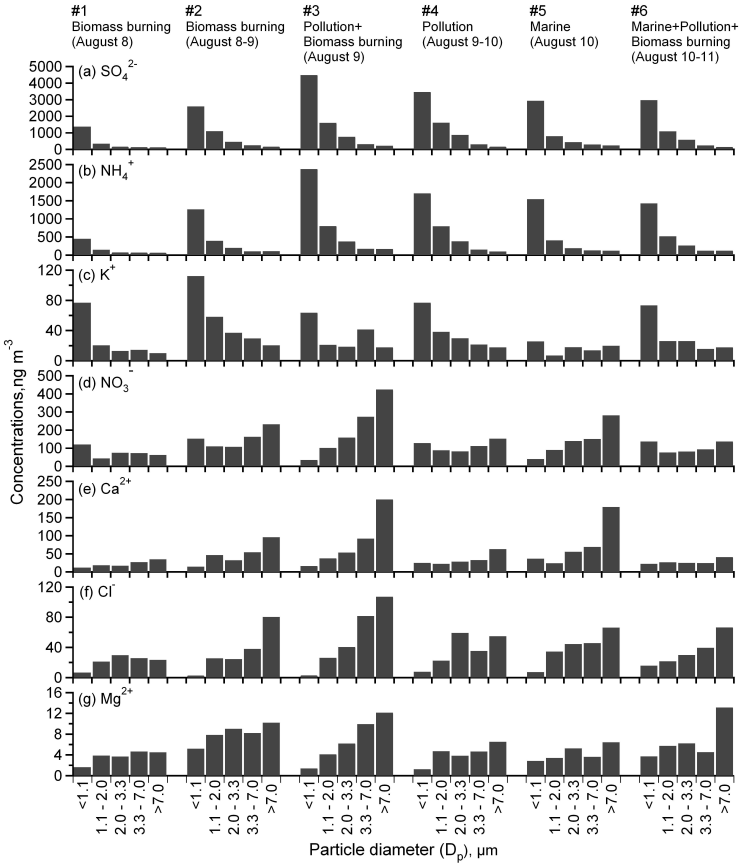

Fig. 7. Size distributions of individual inorganic ions in the Sapporo aerosols collected in summer, 2005.

ACPD
10, 6713–6754, 2010

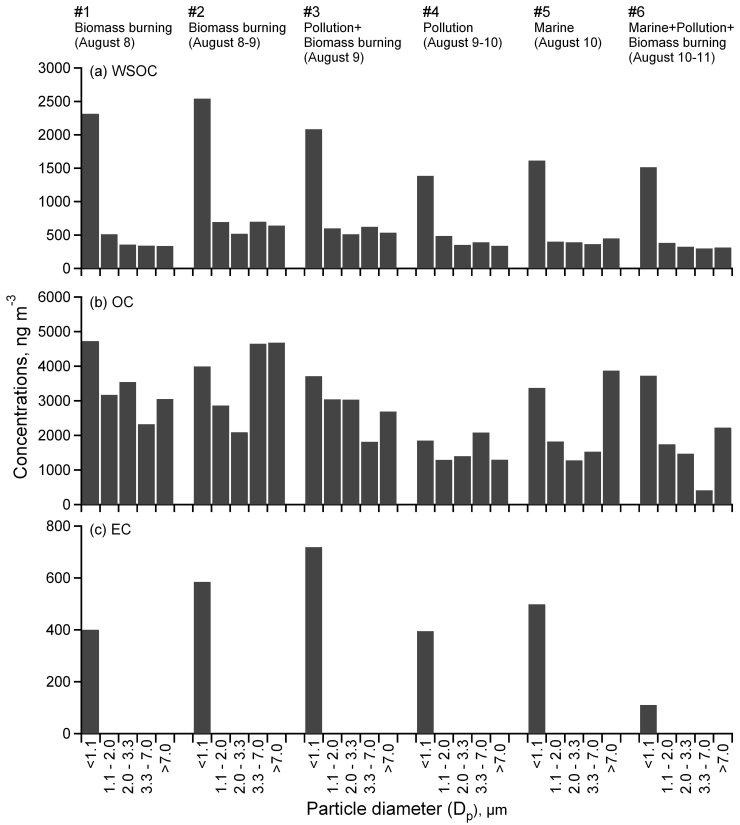

Fig. 8. Size distributions of carbonaceous species in the Sapporo aerosols collected in summer, 2005.

ACPD
10, 6713–6754, 2010

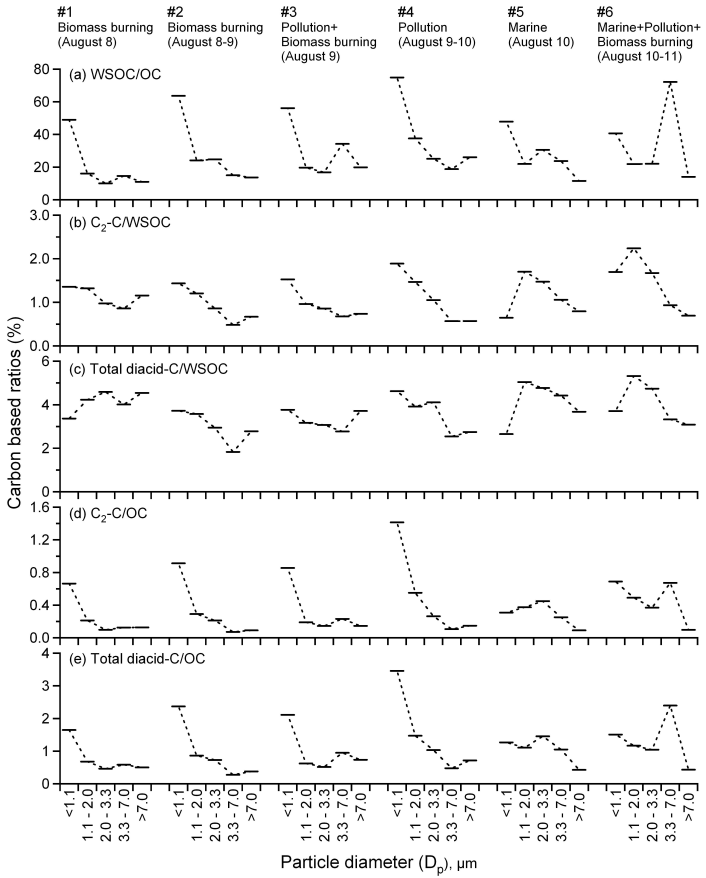

Fig. 9. Size-segregated ratios of **(a)** WSOC/OC, **(b)** oxalic acid-C/WSOC, **(c)** total diacid-C/WSOC, **(d)** oxalic acid-C/OC and **(e)** total diacid-C/OC in the aerosol samples collected during the campaign from 8–11 August 2005 in Sapporo, northern Japan.

ACPD
10, 6713–6754, 2010